Brazilian Journal of Geophysics 43 (2025), 1, 1-32
Brazilian Geophysical Society
ISSN 2764-8044
DOI: 10.22564/brjg.v43i1.2332

OPEN-SYSTEM MAGMATIC EVOLUTION OF THE MORRO DE SÃO JOÃO ALKALINE COMPLEX, SE BRAZIL: INSIGHTS FROM MAGNETOMETRIC SIGNATURES COMBINED TO PETROGRAPHIC ANALYSIS

Mariana Bessa Fagundes[1]*, André Luis Albuquerque dos Reis[2], Anderson Costa dos Santos[1], Mauro Cesar Geraldes[1], Sérgio de Castro Valente[3], Jailane de Sousa Gomes[1]

[1]Universidade do Estado do Rio de Janeiro - UERJ, Rio de Janeiro, RJ, Brazil
[2]Observatório Nacional - ON/MCTI, Rio de Janeiro, Brazil
[3]Universidade Federal Rural do Rio de Janeiro - UFRRJ, Seropédica, RJ, Brazil

Fagundes, M. B. - https://orcid.org/0000-0002-6796-0626
Reis, A. L. A. - https://orcid.org/0000-0002-2225-5106
Santos, A. C. - https://orcid.org/0000-0003-2526-8620
Geraldes, M. C. - https://orcid.org/0000-0003-2914-2814
Valente, S. C. - https://orcid.org/0000-0002-7467-672X
Gomes, J. S. - https://orcid.org/0000-0002-6276-2284

*Corresponding author: marianafbessa@gmail.com

ABSTRACT. The present study integrates the magnetometric with petrographic data from the Morro de São João (MSJ) Alkaline Complex to investigate the magmatic evolution of the complex. The findings emphasize the critical role of magma mixing processes in shaping the textural and compositional diversity of MSJ rocks. The complex is a circular and conical body of approximately 10 km² located southeast of Rio de Janeiro composed of alkaline rocks strongly-silica undersaturation. The study used conventional petrographic analysis and aeromagnetic data processing, such as the Total Gradient Amplitude (TGA) and Reduction to the pole (RTP) maps to reveal the presence of multiple anomalous domains, supporting the hypothesis of non-cogenetic magmatic bodies that interacted during magma mixing events. To accomplish these objectives, this study employs a cross-correlation method to estimate the magnetization direction of the magnetic source. From a geodynamic perspective, the evolution of the MSJ's evolution is supposed to be closely linked to geomagnetic polarity reversals, mantle plume activity, and extensional tectonic processes associated with the break-up of the Gondwana paleocontinent. These factors contributed to the generation of alkaline magmatism through the decompression of the subcontinental lithospheric mantle and the thermal influence of deep mantle plumes.

Keywords: igneous petrology, magmatic system, poikilitic texture, cross-correlation method, magnetization direction of magnetic sources

INTRODUCTION

Aerogeophysical methods are used on every conceivable scale and for a wide range of purposes (Sharma, 1987; Dutra et al., 2022). Among these methods, magnetic surveys are crucial for various applications, including the study of tectonic settings, exploration of minerals and hydrocarbons, groundwater analysis, and geothermal resource assessment (Telford et al., 1990; Nabighian et al., 2005). Recent studies show that the integration of magnetometric data with petrological analyses significantly enhances the interpretation and understanding of magmatic systems. For instance, magnetic measurements have been employed to monitor volcanic activity by tracing subsurface magma movements, providing critical insights into magmatic processes (Magee et al., 2018; Hill et al., 2023).

With this context in mind, the present study investigates the geophysical and petrographic evidence of an open-system behavior during the magmatic evolution of the Morro de São João Alkaline Complex (MSJ). The MSJ, of Cenozoic age, is a circular geological formation measuring approximately 4 km in diameter. It has a conical shape with a top dissected by weathering processes and a summit reaching around 700 m in height. Its landscape is so striking that it is popularly known in the region as the “Casimiro Volcano”. This complex is situated in Casimiro de Abreu, in the southeastern region of Rio de Janeiro (Figure 1). It comprises rocks with alkaline felsic and mafic affinities and exhibits notable magmatic mixing features (Brotzu et al., 2007; Fagundes et al., 2024).

Applications of aeromagnetic data at Morro de São João

Recently, Sales and Martins (2024) applied aerogeophysical technique to focus primarily on delineating the architecture and dynamics of the underlying magma chamber systems for MSJ Alkaline Complex, shedding light on the mechanisms driving magmatic and tectonic developments regionally. To achieve these goals, Sales and Martins (2024) employed methods such as Reduction to the pole (RTP), Total Gradient Amplitude (TGA) in an attempt to enhance the signal from shallow-seated sources, thereby providing maps suitable for interpreting the edges of the sources.

Furthermore, despite the limitations inherent in each method when describing potential fields, the authors included the Upward continuation to attenuate shallow sources; Tilt derivative to normalize the data intensity; the Euler Deconvolution to estimate the position of the sources. Finally, Sales and Martins (2024) constructed a 3D voxel-based inversion to estimate the geometry of the causative source. It is important to note that, in all the steps aforementioned, the authors did not incorporate any prior knowledge about physical properties of the sources, neither in the inversion process nor in the magnetic data processing, such as RTP, which depends on the magnetization direction.

Unlike previous studies, this research employs processing methods based on Total Gradient Amplitude (TGA) and Reduction to the Pole (RTP), incorporating information about a key physical property - the total magnetization direction - of the local source over the MSJ Alkaline Complex. The method relies on the cross-correlation between TGA and RTP to estimate the total magnetization direction. Using this estimated direction, the RTP and TGA maps are constructed, and the study combines these geophysical interpretations with petrographic results to offer valuable insights into the

geology and magmatic processes of the MSJ. Finally, the goal of this work is to enhance our understanding of the local magma chamber system, contributing to the knowledge of both the complex's formation and the regional tectonic evolution. It is important to emphasize that this study does not provide insights into the magnetization evolution (the process of acquisition and the different processes of magnetization over the time) of the MSJ Alkaline Complex. Instead, the total magnetization direction is only used to process the aeromagnetic data and interpret the resulting maps combined with petrographical interpretations. Further details are provided in the following sections.

Geological settings

The Late Cretaceous and Paleocene alkaline magmatism of the South American Platform comprises a series of alkaline provinces in southeastern Brazil, collectively referred to as the Serra do Mar Alkaline Province (PASM - Almeida, 1983). Riccomini et al. (2004, 2005) divided the PASM into two provinces based on the structural control of the magmatic bodies and variations in their ages.

One of these provinces, previously known as the Cabo Frio Magmatic Alignment (Sadowski and Dias Neto, 1981; Almeida, 1991), was later renamed as Poços de Caldas-Cabo Frio Alkaline Alignment (PCCF - Riccomini et al., 2005). This alignment extends from southern Minas Gerais to the coastal region of Rio de Janeiro state.

The PCCF exhibits a structural trend oriented WNW-ESE and includes a series of predominantly felsic alkaline plutons. In addition to the plutons, subvolcanic structures such as sills and dikes, both mafic and felsic, are scattered along the alignment and intrude primarily into the gneissic rocks of the Ribeira and Brasília Orogens (Valeriano et al., 2011; Tupinambá et al., 2012; Alves et al., 2016). The Morro de São João Complex (MSJ) is located at the easternmost of PCCF, intruded into the Cabo Frio Terrain, Ribeira Orogeny. In addition to being north of the Cabo Frio High (CFH), west of the Campos Basin and the Barra de São João Graben, the eastern limit of the Continental Rift of Southeastern Brazil (CRSB - Mohriak et al., 2022 - Figure 1 -).

The evolution of the Cabo Frio Terrane involves episodes of high-grade deformation and metamorphism associated with the collision of continental blocks during the Neoproterozoic (Heilbron et al. (2004). Magmatism in the Cabo Frio Terrane is marked by syn- and post-orogenic granitic intrusions, migmatites from crustal partial melting, and mafic dikes with mantle-derived tholeiitic compositions, reflecting tectonic processes from the Brasiliano Orogeny to Gondwana's fragmentation (Schmitt et al., 2004; Heilbron et al., 2016). Quaternary sedimentary deposits in coastal and alluvial regions document erosional and sedimentary dynamics linked to sea-level changes during the Quaternary (Heilbron et al., 2016).

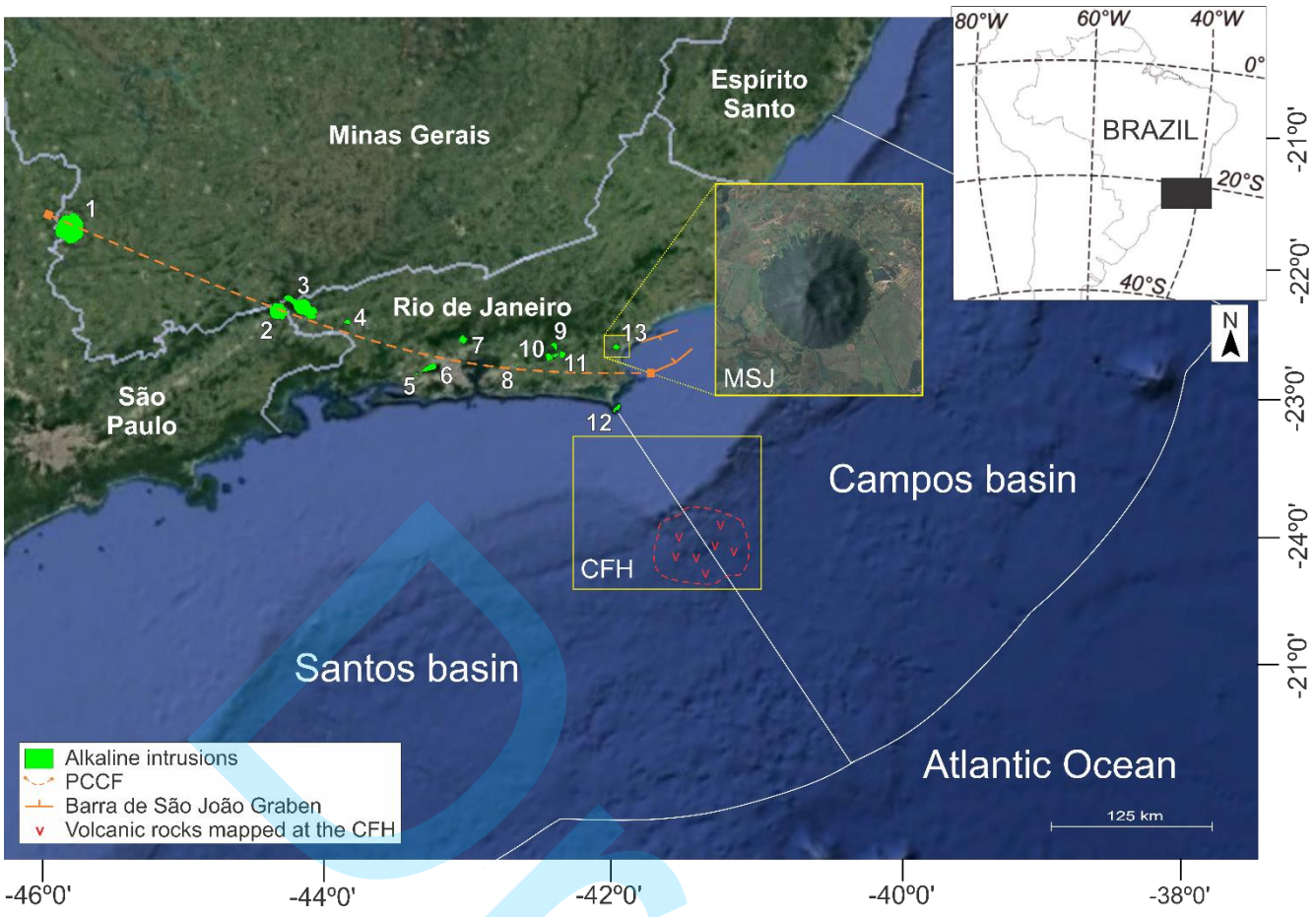

Figure 1: Schematic figure of the location of the MSJ in relation to the PCCF, CFH and Campos Basin. The white lines represent the boundary of the offshore sedimentary basins. The green color indicates the alkaline intrusions of the PCCF: 1) Poços de Caldas (74.6 Ma - $^{40}K/^{40}Ar$ - Ulbrich et al., 2003); 2) Passa Quatro (66.7 Ma - $^{40}K/^{40}Ar$ - Sonoki and Garda, 1988); 3) Itatiaia (70 Ma - U-Pb - Rosa and Ruberti, 2018); 4) Morro Redondo (74.3 Ma - $^{40}K/^{40}Ar$ - Mota, 2012); 5) Marapicu (80 Ma - $^{40}Ar/^{39}Ar$ - Mota, 2012); 6) Mendanha (64, 1 Ma - $^{40}Ar/^{39}Ar$ - Mota, 2012); 7) Tinguá (67.9 Ma - $^{40}K/^{40}Ar$ - Sonoki and Garda, 1988); 8) Itaúna (64.4 Ma - $^{40}K/^{40}Ar$ - Sonoki and Garda, 1988); 9) Soarinho (62 Ma - $^{40}K/^{40}Ar$ - Sonoki and Garda, 1988); 10) Tanguá (68.4 Ma - $^{40}K/^{40}Ar$ - Sonoki and Garda, 1988); 11) Rio Bonito (68.4 Ma - $^{40}K/^{40}Ar$ - Sonoki and Garda, 1988); 12) Ilha de Cabo Frio (68.4 Ma - $^{40}K/^{40}Ar$ - Motoki et al., 2013); 13) Morro de São João (64.8 Ma $^{40}K/^{40}Ar$ – Mota, 2012). Modified from Almeida et al. (2013); Heilbron et al. (2016); Mohriak et al. (2022), Barros et al. (2023), and Fagundes (2024).

MATERIALS AND METHODS

Field Campaign

For the preparation of geological maps, the topographic bases were sourced from the RJ-25 Project database of the IBGE and subsequently processed, adjusted, and edited by the technical team of the Tectonic Studies Laboratory (LET) at Rio de Janeiro State University (UERJ), using ArcGIS 10.6 software.

The field campaigns were divided into three stages. The first stage focused on the eastern and southeastern sectors of the complex, based on an initial interpretation of geomorphological characteristics and descriptions of the local lithology. During the second stage, mapping efforts were concentrated on the southern, southwestern, and western sectors, with sampling points primarily located along the road encircling the body. The third stage was exclusively dedicated to delineating the predominance of facies to define contacts and construct the geological map. The central part of the complex requires more elaborate logistics and mapping methods due to several challenges. In addition to being located on private properties that control access to the main trails leading to the central region, it is covered by dense vegetation (Mata Atlântica biome). Furthermore, it was previously an area of illegal hunting, with numerous traps installed throughout, which limits entry, handling, and any human interventions, while posing significant risks to those entering the complex.

In total, 94 samples were collected during four field campaigns across the complex, of which 89 were selected for petrographic analysis.

Petrography

The processes of thin section preparation and sample polishing were conducted at the Laboratório Geológico de Preparação de Amostras (LGPA) at the Rio de Janeiro State University (UERJ) and by the contracted company SOLINTEC – Serviços em Geologia Integrados, respectively.

Petrographic thin sections were examined under transmitted light using a conventional petrographic microscopy on a Zeiss Axioskop 40 microscope. The investigation involved semi-quantitative analysis based on the average modal proportions obtained from approximately 8 to 10 fields of view for each thin section. The classification criteria for macroscopic descriptions followed the standards established by the Subcommission on the Systematics of Igneous Rocks of the International Union of Geological Sciences (IUGS), as outlined by Streckeisen (1976) and Le Maitre (2002).

Geophysical data processing

The field data used here was obtained from an aeromagnetic survey carried out in the state of Rio de Janeiro and provided by the Geological Survey of Brazil (Serviço Geológico do Brasil - SGB) of the Aerogeophysical Project 1117 - Rio de Janeiro (CPRM, 2012), available in XYZ format on the GEOSGB (2022) online platform. The survey covers an area of approximately 32,000 km^2 between the latitudes from - 20º to - 23° and longitudes from - 44° to - 41.5° referred to in the WGS-84 datum. The flight height was 100 m above the ground. The inlines and tie lines are spaced at 500 m and 10 km with orientation along with N-S and E-W, respectively. For the MSJ application, we crop an area limited to latitudes from - 22.5° to - 22.6° and longitudes from - 42.01° to - 42.06°, totalizing a number of 38,000 observations. The main geomagnetic field direction at the epoch of survey for this area was equal to - 39.06° and - 22.71º for inclination and declination, respectively.

Reduction to the pole (RTP) and the total gradient amplitude (TGA) computation

Different from gravity data, where the anomalies tend to be located over the causative sources, the total-field anomaly (TFA) depends on the main field (*i.e.,* the geomagnetic field) and the total magnetization directions. This fact leads to a phase shift contribution in the magnetic data, mainly when the ambient field and the magnetization direction do not have the same direction. For this reason, it may distort the shape of the anomaly or even change its sign. In general terms, the magnetic anomaly depends on the direction of the geomagnetic field at the epoch of the survey and depends on a vectorial summation of other two components: the induced magnetization (i.e., the response of the source to an ambient field) and the natural remanent magnetization (*i.e.,* the component acquired at the time of the rock formation). This complexity can be attenuated by applying a phase transformation called Reduction to the Pole (RTP). This technique was first introduced by Baranov (1957). The RTP transformation leads to an anomaly that would be measured at the north magnetic pole, where the source would have purely vertically induced magnetization. In other words, it will transform a measured total-field anomaly into the vertical component of the field caused by the same source distribution magnetized in the vertical direction. This transformation relocates the anomaly over the magnetic source, making the interpretation process more suitable. It is commonly performed in Fourier Domain by applying an RTP filter. Nevertheless, this process depends on the magnetization direction of the sources and, consequently, we have to estimate this physical property. However, as with any other technique, there are some limitations (Blakely, 1996, p. 330).

The concept of the analytic signal was first introduced by Ville (1948). The analytic signal of a function is a complex quantity that is represented by the Hilbert Transformation of an arbitrary function. It was pioneered in potential field data processing by Nabighian (1972, 1974). In this context, the potential field analytical signal is the summation of the horizontal (i.e., the derivative in the x- and/or y-axis direction) and the vertical (*i.e.,* along the z-axis) gradients of a potential field. It leads to a commonly known quantity called Analytic Signal Amplitude (ASA), which is the Euclidean norm of the aforementioned derivatives. For practical purposes, here we used the term Total Gradient Amplitude (TGA) adopted by Reid (2012). The use of TGA may complement the RTP in the interpretation process, and estimating the magnetization direction.

Cross-correlation method for estimating the total magnetization direction

The total magnetization is the sum of two components: the induced and the remanent magnetizations. The induced magnetization of the lithospheric rocks is due to the response of the lithospheric rocks to an ambient field (*i.e.,* the geomagnetic field), which is also known as an induced magnetic field. The remanent magnetization preserves the geological history of rocks and the past Earth's magnetic field, including the magnetization acquisition at the time of formation and the posteriorly processes along the geological time due to metamorphism, for example, the chemical alteration and stress deformation (Dunlop and Özdemir, 1997; Ravat, 2007; Gonzalez et al., 2022). For this reason, the determination of the magnetization direction is a suitable tool for describing the lithospheric rocks and, consequently,

their history throughout time. In the context of applied geophysics, ignoring this physical property can lead to a misinterpretation of the geological scenarios.

Clark (2014) presented a seminal review of available methods for determining the remanent and total magnetization. Due to difficulties in directly estimating the remanent component from total-field magnetic anomalies data, the author emphasizes the importance of indirect methods for estimating the total magnetization direction, which was divided into eight strategies. These groups of methods are the following : (a) constrained modeling and inversion-based methods (*e.g.,* Lelièvre and Oldenburg, 2009; Liu et al., 2017); (b) inversion method assuming, a priori, simple geometries (*e.g.,* Oliveira Jr. et al., 2015); (c) magnetization estimation pre- and post-mining; (d) combined analysis of magnetic and gravimetric anomalies based on Poisson's relation (*e.g.,* Alencar de Matos and Mendonça, 2020); (e) methods based on controlled sources (*e.g.,* Huang and Fraser, 2001); (f) method using Helbig-type integrals (*e.g.,* Tontini and Pedersen, 2008); (g) equivalent-layer technique based estimation (Ribeiro-Filho et al., 2020; Reis et al., 2020) and (h) cross-correlation methods. In this work, we use the last group.

The approach of cross-correlation methods consists of enhancing some symmetry of potential quantities using statistical correlation. The idea consists of estimating the total magnetization direction by searching for the maximum cross-correlation coefficient (*e.g.,* Pearson correlation coefficient) from a grid search of inclinations and declination. There are several methods based on this strategy in the current literature. As a pioneer work, Roest and Pilkington (1993) propose a method for estimating total-magnetization direction by correlating the total gradient amplitude of the RTP field for 2D magnetic sources. Fedi et al. (1994) applied successive RTP operations assuming that the total magnetization direction could be estimated by searching the inclination and declination into a grid. Bilim and Ates (2004) performed the maximum correlation between the gravity field and pseudo gravity from magnetic anomalies that can provide a valuable estimation of the total magnetization. Dannemiller and Li (2006) analyze the correlation between the total and vertical gradients from the RTP field for different magnetization directions. Gerovska et al. (2009) apply the cross-correlation between the magnetic amplitude and RTP anomalies. Li et al. (2017) presented a new cross-correlation method of normalized source strength (NSS) and RTP field by computing a combination of inclinations and declinations. Zhang et al. (2018) extended this approach by applying the correlation between the derivative of the NSS and the RTP field for a set of trial magnetization directions. Ribeiro-Filho et al. (2020) improved the Dannemiller and Li (2006) for the application in low-latitude anomalies by using the cross-correlation between potential quantities calculated from the equivalent-layer technique. Jian et al. (2022) presented a new correlation method by using multiple correlations of potential field quantities. Finally, in this work, we use the cross-correlation between the TGA and RTP fields for estimating the MSJ magnetization direction from total-field anomaly data. The estimated magnetization direction, as well as all magnetic data processing, was determined by developing Python scripts using the Numpy (Harris et al., 2020) and Scipy (Virtanen et al., 2020) libraries.

RESULTS

MSJ features and structures

.

The complex stands out in the landscape due to its peak of approximately 700 m above sea level. The drainage system in the MSJ is of the radial, centripetal, and centrifugal type. There are no conventional in situ outcrops in the MSJ. However, deposits of talus and metric-scale blocks, mainly within the drainages of the body, were used for sampling (Figure 2B). Rocks belong to the gneissic basement of the Cabo Frio Terrain, Ribeira Belt, and outcrops in the road cuts as regolith (Figure 2C).

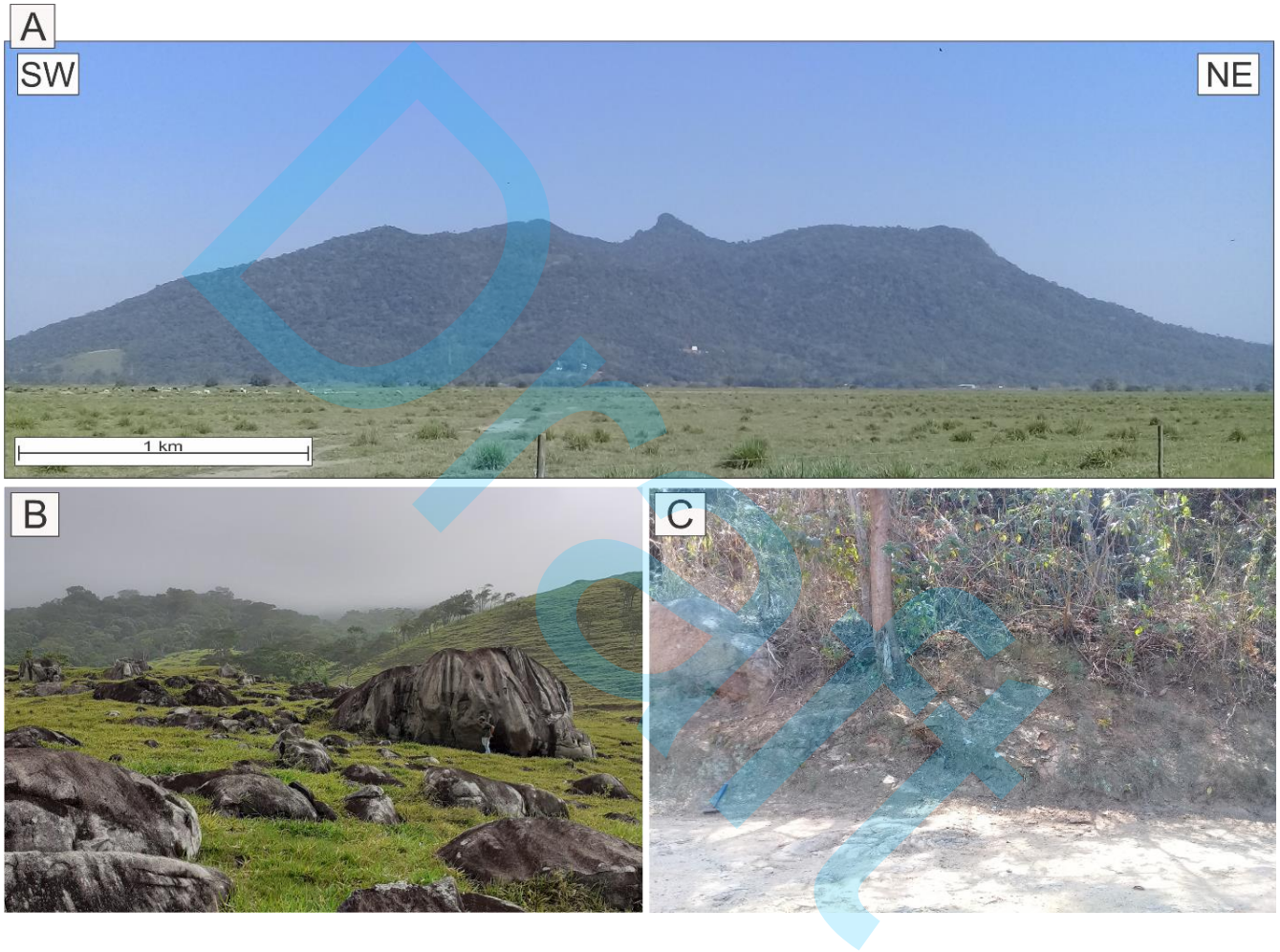

Figure 2: Main features of the MSJ. A) Panoramic view of the complex; B) Thallus deposit, typical feature; C) Road cut with regolith from the crystalline basement.

Tabular structures, essentially felsic, are observed in all sectors of the complex (Figure 3A). Due to the lack of structural data and the absence of in situ outcrops, these structures cannot be definitively classified as dikes or sills; therefore, they are referred to in this manner. These structures vary in thickness on a centimeter scale and are associated with all the rocks present in the complex.

Three critical structures were observed in the field: (1) interaction between materials of different compositions. This feature is composed of mafic and felsic rocks and has varying centimeter sizes with

abrupt and polygonal contacts (Figure 3B) or corroded with a diffuse interaction between the two distinct rocks; (2) xenoliths of gneissic rocks (Figure 3C). The xenoliths are approximately 15 to 20 cm in size and have polygonal contacts; and (3) enclaves (Figure 3D) of ultramafic rock with a rounded shape, approximately 15 cm in diameter. The enclaves are only observed in the mafic rocks of the complex.

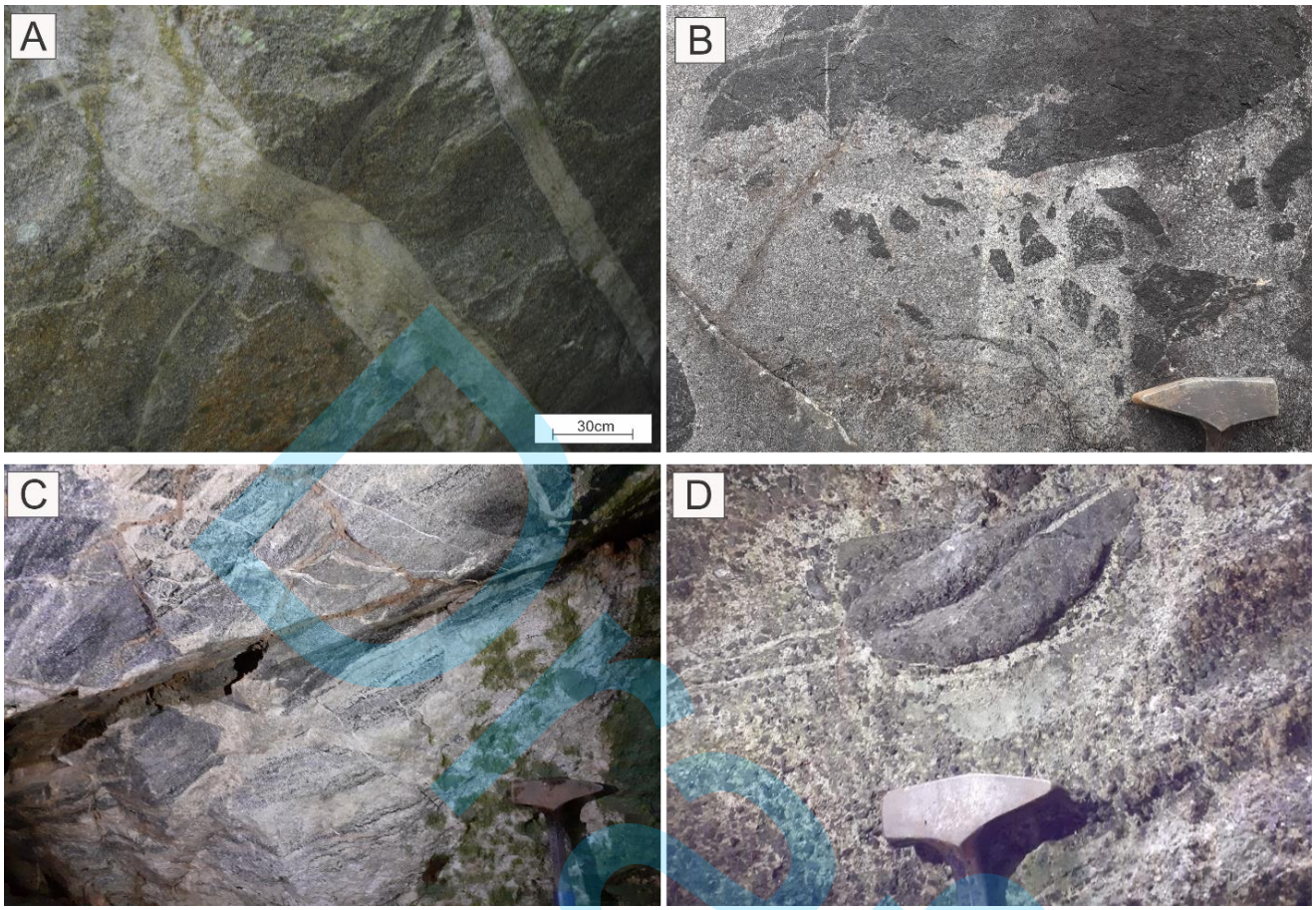

Figure 3: Structures observed in the MSJ rocks. A) Tabular structures; B) Interaction features of magmas of different compositions; C) Xenoliths of the host rock; D) Ultramafic enclave hosted in a mafic rock.

Petrography

Except for the aphanitic hypabyssal rocks, the rocks within the complex are predominantly phaneritic, holocrystalline, inequigranular, and medium- to coarse-grained. The essential mineralogy consists of alkali-feldspar, plagioclase, nepheline, clinopyroxene, and amphibole, as well as accessory titanite, apatite, garnet, titanomagnetite, subordinate, biotite, carbonate, sulfide, cancrinite, and zircon. Based on their mineralogical composition and textural characteristics, the MSJ rocks are classified as nepheline-bearing alkali-feldspar syenite, nepheline syenite, nepheline-bearing syenite, nepheline monzosyenite, malignite, shonkinite and essexite, as well as phonolites.

Felsic Rocks

The nepheline-bearing alkali-feldspar syenite exhibits a serial inequigranular texture, characterized by

tabular alkali-feldspar crystals with semi-polygonal edges and subhedral nepheline, which is occasionally altered to cancrinite. This texture results from the coexistence of two alkali-feldspar populations with grain sizes ranging from fine to medium. Essential minerals include nepheline, alkali-feldspar, and clinopyroxene, the latter appearing as anhedral crystals with serrated edges and greenish hues. Accessory minerals include brownish prismatic titanite, Fe and Ti oxides, and anhedral garnet with compositional zoning (Figure 4A) and brown hues. Additionally, sodalite and alteration minerals such as sericite are occasionally observed.

The nepheline syenite and nepheline-bearing syenite share similar inequigranular textures, with tabular alkali-feldspar crystals exhibiting semi-polygonal edges and subhedral nepheline. The primary distinction between the two is the modal content of nepheline, which is higher in the nepheline-bearing syenite. Clinopyroxene in these rocks displays greenish and brown hues and is often overgrown by amphibole (Figure 4B), appearing as anhedral crystals with serrated edges. Accessory minerals include titanite, garnet, Fe and Ti oxides, zircon, and sodalite, with the garnet showing irregular compositional zoning in various shades of brown. These garnet crystals are granular, medium to coarse-grained, and occasionally contain alkali-feldspar inclusions.

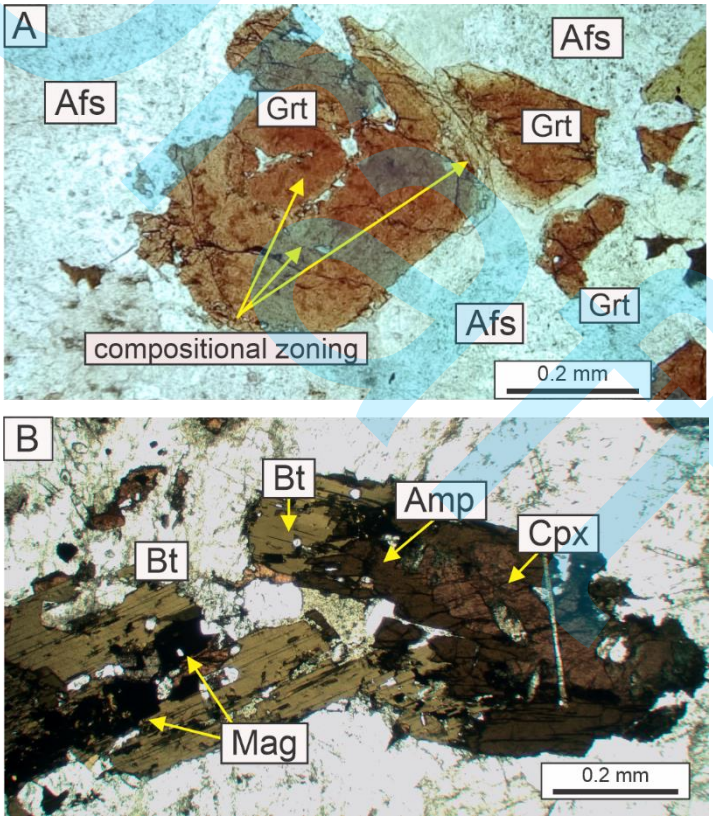

Figure 4: Photomicrograph showing predominant mineral textures in the felsic rocks of the MSJ. (A) Garnet (Grt) crystal with strong compositional zoning in the brown colors of an nepheline-bearing alkali-feldspar (Afs) syenite; (B) clinopyroxene (Cpx) crystal overgrown with amphibole (Amp) and also associated with biotite (Bt) from a nepheline syenite. Mag: Fe and Ti oxide.

The nepheline monzosyenite is associated with magmatic mixing structures commonly found within the complex. These rocks exhibit an inequigranular, mesocratic texture due to the modal abundance of clinopyroxene and amphibole. Alkali-feldspar and nepheline occur as medium-grained, anhedral to subhedral crystals, sometimes interstitially associated with mafic minerals. Amphibole overgrowth on clinopyroxene is a notable feature, although fine-grained, subhedral clinopyroxene crystals without overgrowth are also present. These crystals display compositional zoning with green and brown hues, characterized by three distinct patterns: irregular zoning (Figure 5A) with random alternation of green and brown hues, concentric zoning (Figures 5B and C) with brown cores and green rims, and concentric zoning with green cores and brown rims. Accessory minerals in these rocks include anhedral garnet, prismatic titanite, globular and acicular apatite, Fe and Ti oxides, zircon, fine-grained mica, and zircon. These accessory minerals are often associated with the amphibole overgrowth on clinopyroxene.

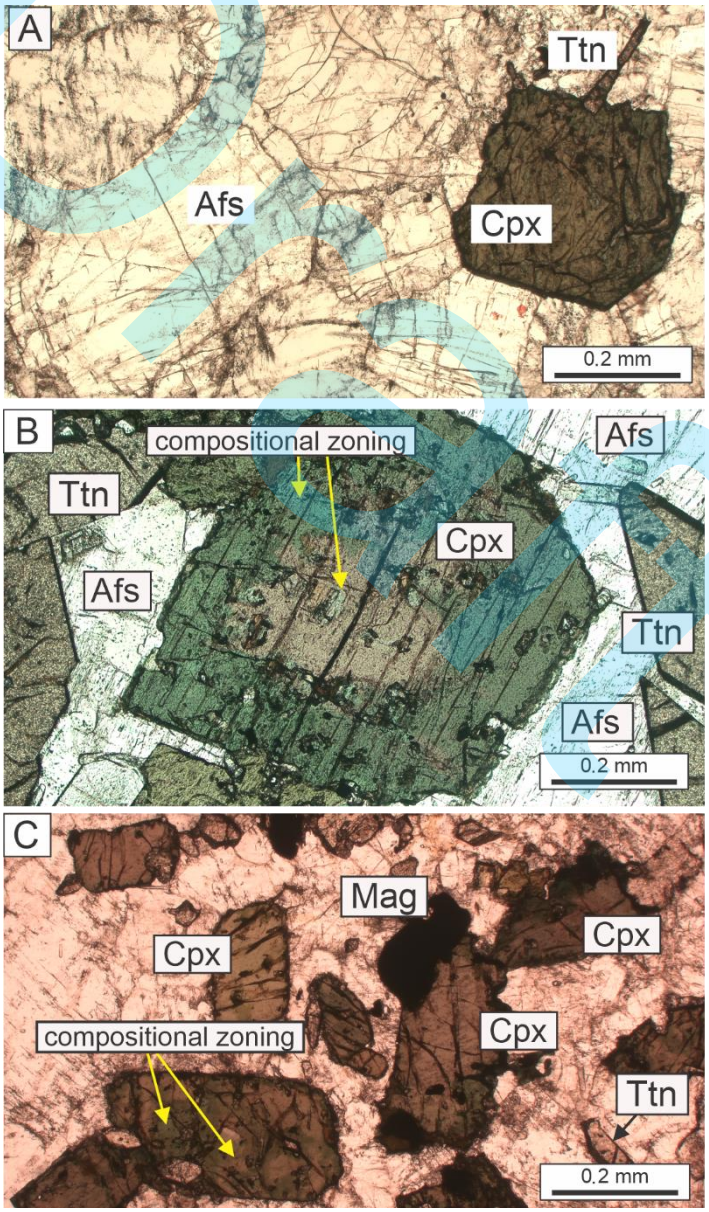

Figure 5: Photomicrograph exhibiting the textural variations of the clinopyroxene (Cpx) crystals found in the nepheline monzosyenite rocks of the MSJ. A) Clinopyroxene with irregular compositional zoning; B) Clinopyroxene with concentric zoning with brown centers and green edges; C) Clinopyroxene with subtle compositional zoning, displaying green cores and brown rims, associated with Fe-Ti oxides (Mag) and titanite (Ttn). Afs: alkali-fedspar.

Phonolites have a mineralogy composed of alkali-feldspar, nepheline, amphibole, clinopyroxene and fine-grained Fe and Ti oxides. In the massive phonolite, the fine-grained alkali-feldspar are oriented, generating a moderate flow texture. In porphyry phonolites, the matrix does not have a preferential crystalline orientation and alkali-feldspar, nepheline, which sometimes displays a glomeroporphyritic texture, and medium-grained sodalite make up the phenocrysts of these rocks.

The following Table 1 summarizes the relevant characteristics of each rock, presenting them in terms of texture, main minerals, accessory minerals, and key features.

Table 1. Comparative table between the felsic rocks of Morro de São João.

Rock	Texture	Main minerals	Accessory minerals	Key features
Nepheline-bearing alkali-feldspar syenite	Serial inequigranular; fine-to medium-grained	Alkali-feldspar (tabular), nepheline (subhedral, altered to cancrinite) and clinopyroxene overgrown by amphibole	Titanite (prismatic), Fe and Ti oxides, garnet (zoned, brown), sodalite, sericite, zircon	Two alkali-feldspar populations; greenish clinopyroxene overgrown by amphibole
Nepheline syenite and nepheline-bearing syenite	Inequigranular	Alkali-feldspar (tabular), nepheline (subhedral) and clinopyroxene overgrown by amphibole	Titanite, garnet (zoned, irregular, brown), Fe and Ti oxides, sodalite, zircon	Garnet with alkali-feldspar inclusions; clinopyroxene overgrown by amphibole (greenish to brown tones)
Nepheline monzosyenite	Inequigranular	Alkali-feldspar, nepheline, clinopyroxene (zoned) and clinopyroxene overgrown by amphibole	Garnet, titanite, apatite (globular/acicular), Fe and Ti oxides, mica, zircon	Three clinopyroxene zoning patterns; associated with magmatic mixing structures
Phonolite	Massive	Alkali-feldspar	Oxide, garnet and clinopyroxene	Fine-grained crystals of clinopyroxene, nepheline and oxide are found in the matrix
	Glomeroporphyritic	Phenocrysts: alkali-feldspar, nepheline and sodalite Matrix: alkali-feldspar	Oxide, garnet and clinopyroxene	

Mafic rocks

Malignite and Shonkinite exhibit a serial inequigranular texture with a bimodal size distribution, comprising fine-grained anhedral crystals and medium-grained subhedral alkali-feldspar crystals.

Anhedral nepheline, medium-grained, is present throughout the rocks. Clinopyroxene displays compositional zoning with green and brown hues, appearing as fine-grained, subhedral crystals. Some clinopyroxenes exhibit overgrowths of amphibole with serrated edges and medium to coarse grain sizes. Amphibole is also found as anhedral, coarse-grained, dark brown crystals with a poikilitic texture (Figure 6A), often containing inclusions of clinopyroxene, Fe and Ti oxides, and alkali-feldspar. Rare subhedral brown amphibole crystals without a cumulate texture are occasionally observed (Figure 6B).

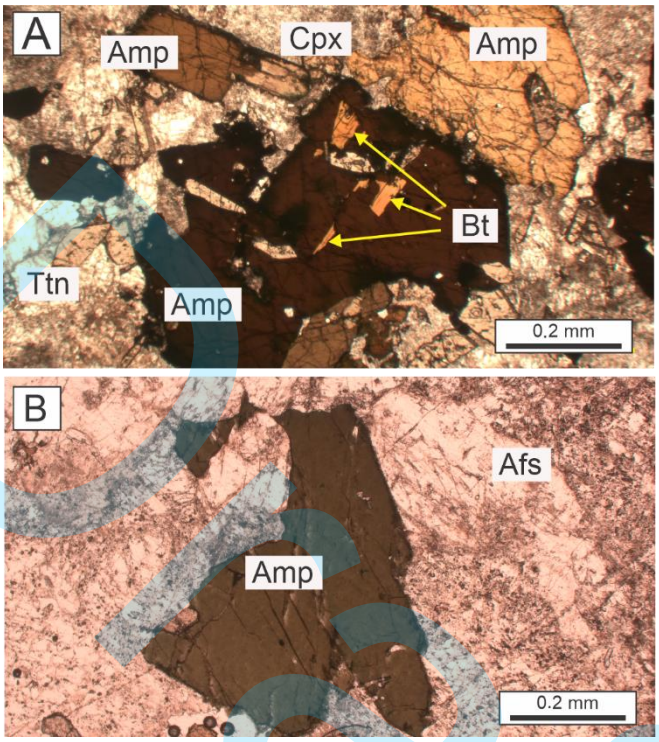

Figure 6: Photomicrograph exhibiting the textural variations of the amphibole (Amp) crystals in the malignite. A) Amphibole with poikilitic texture with clinopyroxene (Cpx) and biotite (Bt) as included crystals; B) Rare amphibole crystal found in the MSJ mafic rocks without poikilitic texture. Afs: alkali-feldspar.

Essexite contains dark brown amphibole macrocrystals with a poikilitic texture and clinopyroxene showing pronounced green and brown compositional zoning. The clinopyroxene crystals are fine-grained and subhedral, while the felsic phase predominantly consists of alkali-feldspar, plagioclase and nepheline. Accessory minerals include garnet, titanite, Fe and Ti oxides, apatite, and zircon.

Essexite with cumulatic texture commonly display oriented arrangements of clinopyroxene and amphibole with poikilitic textures. In these rocks, interstices are filled with alkali-feldspar and nepheline. In non-cumulate-textured essexites, fine- to medium-grained felsic minerals exhibit subhedral and truncated contacts, while other mineral features are consistent with cumulate-textured rocks. Apatite is present in all rocks of the MSJ. In cumulate-textured rocks, apatite appears prominently in interstitial

spaces and as inclusions within poikilitic textures, where it is predominantly acicular.

The following Table 2 summarizes the relevant characteristics of each rock, presenting them in terms of texture, main minerals, accessory minerals, and key features.

Table 2. Comparative table between the mafic rocks of Morro de São João.

Rock	Texture	Main minerals	Accessory minerals	Key features
Malignite and Shonkinite	Serial inequigranular	Clinopyroxene (zoned green/brown, subhedral), clinopyroxene overgrown by amphibole, nepheline (anhedral, medium-grained), and alkali-feldspar	Titanite, Fe and Ti oxides, alkali-feldspar, apatite, and zircon	Amphibole with poikilitic texture includes clinopyroxene, Fe and Ti oxides, alkali-feldspar
Essexite	Cumulatic	Clinopyroxene (zoned green/brown, subhedral), amphibole (brown, subhedral to poikilitic)	Garnet, titanite, Fe and Ti oxides, apatite, and zircon	Amphibole with poikilitic texture includes clinopyroxene, Fe and Ti oxides, alkali-feldspar; rare subhedral brown amphibole
	Massive	Clinopyroxene (zoned green/brown, subhedral), amphibole (brown, subhedral to poikilitic), nepheline (anhedral, medium-grained), and alkali-alkali-feldspar		Cumulate rocks feature poikilitic amphibole and interstitial acicular apatite

Magnetic data processing and total magnetization direction estimation

The raw total-field anomaly data (not shown) were interpolated into a grid of 600 x 12 (7200 points) with a grid spacing of 49 m and 502 m, respectively, along with northing and easting directions. The gridded total-field anomaly data is shown in Figure 7A. We processed the gridded data for a regional-residual separation. With this purpose, we used a first-order polynomial fitting to the gridded data (Figure 7B).

After removing the regional field (Figure 7B) from the gridded data (Figure 7A), we obtained the residual field shown in Figure 7C. In order to estimate the total magnetization direction, we applied the

cross-correlation method by correlating RTP and TGA calculated from the residual total-field anomaly. We construct a grid of trial orientations ranging the inclinations from 5° to 90° and the declinations from -180° to 180° with an increment of 0.5° for both. The grid search is shown in Figure 7D. We set a maximum correlation equal to 0.51. This value corresponds to a total magnetization direction of 57.5° and -79.5 for inclination and declination, respectively, which is characterized as a reversed magnetization. The reason for reaching this conclusion is that when the magnetization is opposed to the direction of the present day field (*i.e.*, the main field direction), it is referred to as reverse magnetization (for more details see Mazaud, 2007). It can be observed by the difference between the sign of the inclination of the main field and the sign of the estimated total magnetization inclination obtained by the method.

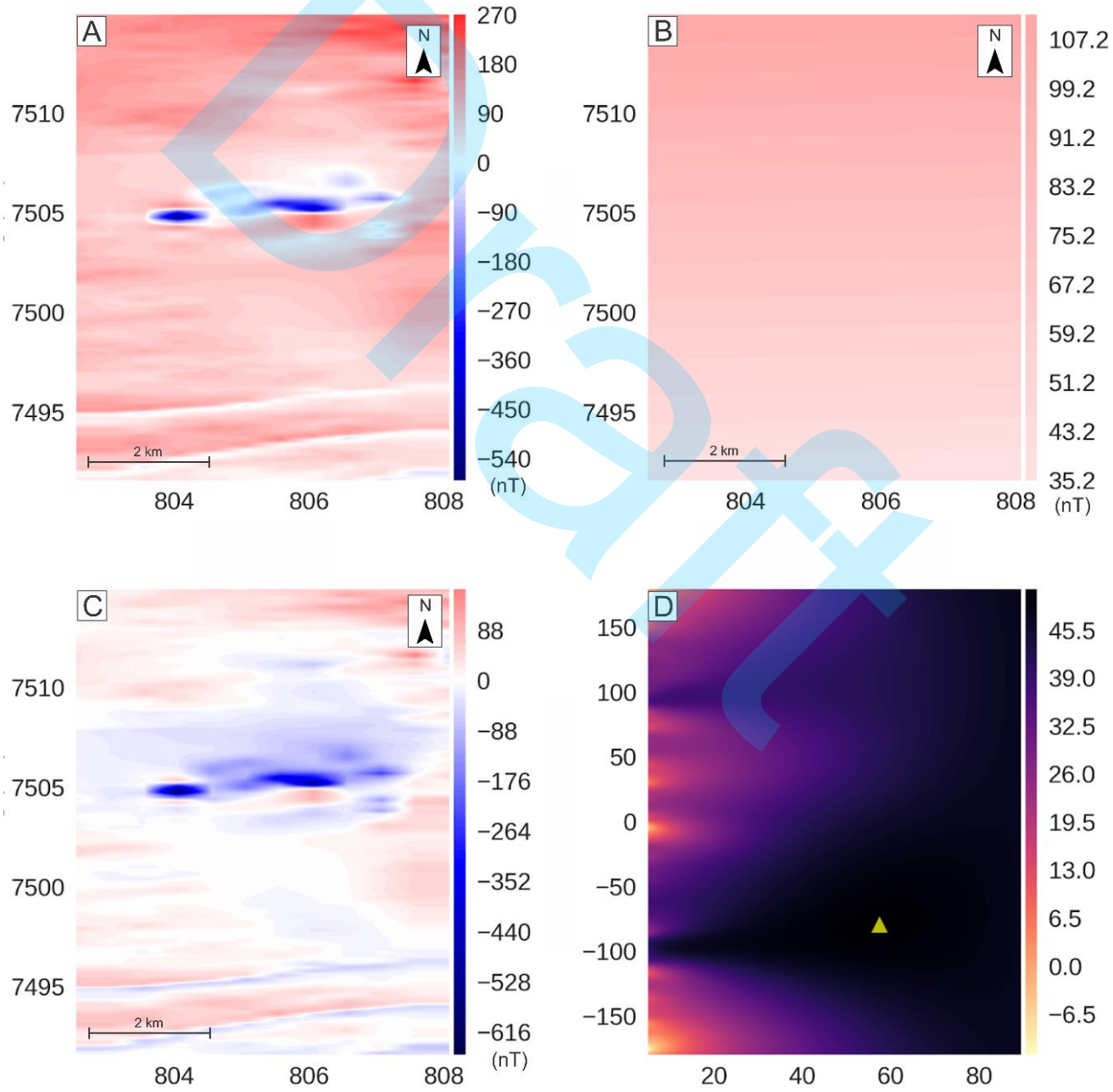

Figure 7: Results for processing and total magnetization direction estimation of MSJ area. A) Gridded TFA (nT) from the raw anomaly data (not shown); B) Regional field (nT) estimated from a first-order polynomial fitting; C) Residual total-field anomaly (nT), obtained subtracting panels (A) and (B); D) Cross-correlation map, where the yellow triangle shows the maximum correlation between RTP and TGA data which gives the estimation of total magnetization direction. In the figure, the axes of the maps in A, B and C are given in kilometers and the one in D is given in degrees (declination and inclination), respectively.

We used this estimated magnetization direction to perform a RTP and TGA calculation for interpreting the magnetic data (Figure 8). The RTP field (Figure 8A) shows a centered high amplitude above the causative sources, demonstrating that we estimate a reliable magnetization direction. The TGA map (Figure 8B) confirms the high correlation between these two potential quantities, as well as highlighting almost the same structures in both results. These results show that we obtained a reliable result for the magnetization direction, indicating a set of causative magnetic sources mainly into the region composing MSJ (the solid black line in Figure 8A and Figure 8B).

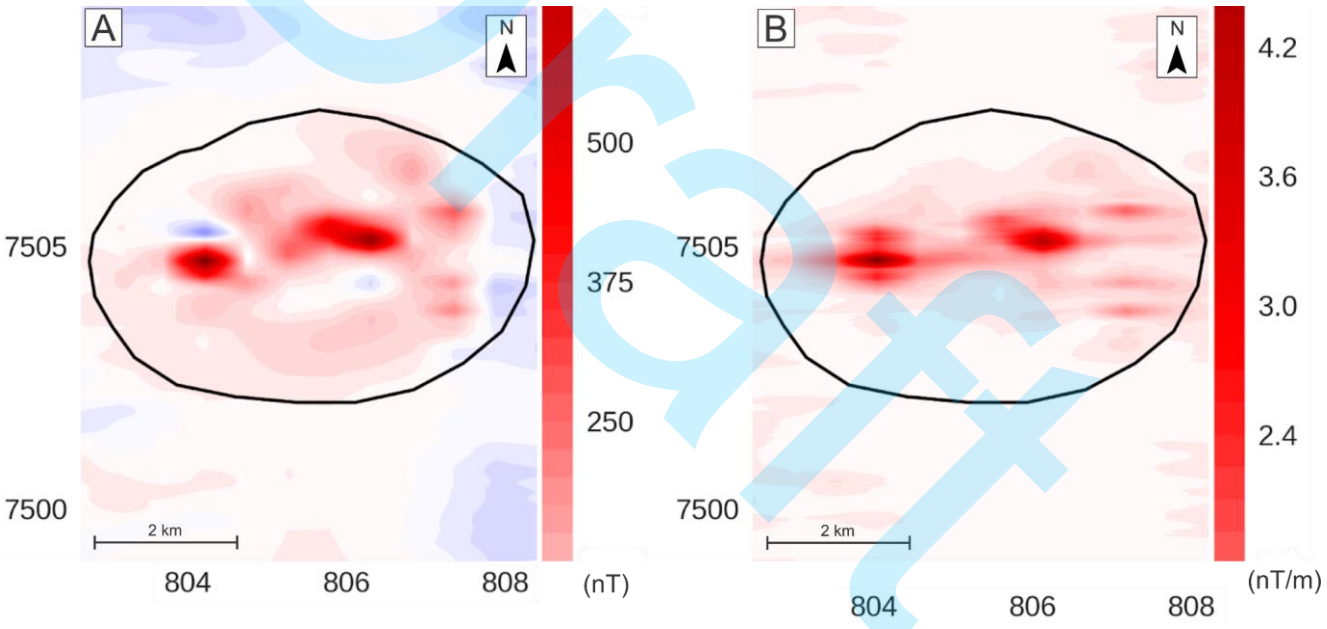

Figure 8: Results for interpreting the causative bodies within the area of MSJ limited by the solid black line in both maps. The color gradient (from light to dark red) indicates variations in the intensity of the magnetic gradient, with higher values associated with areas in darker red (magnetic peaks). A) RTP (nT) anomaly obtained from the magnetization direction estimative; B) TGA (nT/m) field obtained from RTP anomaly.

DISCUSSIONS

Geochronological data (Brotzu et al., 2007; Mota et al., 2009; Fagundes, 2024) indicate that one of the magmatic pulses responsible for the formation of the MSJ occurred approximately 65 Ma. This age

marks the end of the Cretaceous and the beginning of the Paleocene, a period contemporaneous with the establishment of the CRSB (Riccomini et al., 2004, 2005). During this time, magmatic activity (tholeiitic and alkaline) along southeastern Brazil, particularly in the Serra do Mar region, and various dyke intrusions were closely associated with the development of the rift system.

The mafic rocks of the MSJ, such as essexites and malignites, according to Fagundes (2020, 2024), exhibit SiO_2 contents ranging from 39.17 to 46.68 wt.%, are metaluminous, and potassic with a sodic tendency. In contrast, the felsic rocks, represented by nepheline syenite, syenite with nepheline, nepheline monzosyenite, alkali-feldspar syenite with nepheline, and phonolite, exhibit SiO_2 contents ranging from 51 to 55.18 wt.% and MgO contents between 0.14 and 0.92 wt.%. These felsic rocks are potassic to ultrapotassic, metaluminous with a tendency towards peralkaline and peraluminous compositions (Fagundes, 2020, 2024).

According to the aforementioned author, the metaluminous geochemical signature of these rocks is reflected in their mineralogy, while the textures observed in their minerals reflect the magmatic evolution of the complex (Fagundes et al., 2024). The conventional petrographic analysis conducted in the present study, together with the mineral chemistry, elemental geochemistry, and isotopic analyses proposed by Brotzu et al. (2007) and Fagundes et al. (2024) suggest that processes such as crustal assimilation and magma mixing in an open-system played a significant role in the magmatic evolution of the MSJ.

In their work, Azzone et al. (2016), Vlach et al. (2018) and Fagundes et al. (2024) conducted an extensive study of disequilibrium textures observed in clinopyroxene, garnet, and amphibole crystals from the Ponte Nova Alkaline Massif, Poços de Caldas Alkaline Massif and MSJ rocks, respectively. The authors assert that crustal assimilation processes are responsible for the pronounced compositional zoning patterns exhibited by these minerals. However, the present study emphasizes textures that are indicative of magma mixing processes.

Petrological and magnetometric data integration

As a result of the magma mixing process, an important texture was imprinted on amphibole crystals (Fagundes, 2024): the poikilitic texture. Commonly described by Azzone et al. (2016) in the rocks of the Ponte Nova Alkaline Massif, this texture is characteristic of cumulate mafic rocks and occurs in lower modal proportions in non-cumulate mafic rocks of the MSJ.

Latypov et al. (2020) and Mollo and Hammer (2017) associate the formation of poikilitic texture with magma mixing processes involving the cooling and crystallization of magmas with differing compositions and temperatures. Latypov et al. (2020) suggest that poikilitic texture can form through the interaction between crystals from a more primitive (and typically hotter) magma and a more evolved (and cooler) host magma. During this interaction, larger crystals may act as oikocrysts, encapsulating smaller minerals (chadacrysts) or those of differing compositions. This process is driven by chemical instability resulting from magma mixing, which promotes the simultaneous nucleation and growth of various mineral phases.

Mollo and Hammer (2017) similarly associate poikilitic texture with magma mixing, emphasizing that fluctuations in temperature, chemical composition, and flow dynamics during magma interactions create favorable conditions for smaller crystals to be entrapped within larger ones. These conditions are characteristic of magmatic systems where mixing is incomplete, resulting in disequilibrium textures such as poikilitic textures. Thermal and compositional interactions also influence the saturation of minerals in the magma, fostering the crystallization of mineral phases out of equilibrium with the magmatic liquid. Thus, it is possible to state that poikilitic texture serves as a significant petrographic indicator of magma mixing processes. It is frequently employed as evidence of magmatic interactions in intrusive complexes.

The idea that distinct batches of magma mixed at a specific stage in geological time can be associated with observations from the Total Gradient Amplitude (TGA - nT/m) map, where a set of laterally associated anomalous domains is evident. The magnetic domains were delineated using the highest TGA values (Figure 9), with eight peaks identified. These anomalies range from 0.5 to 4.5 nT/m.

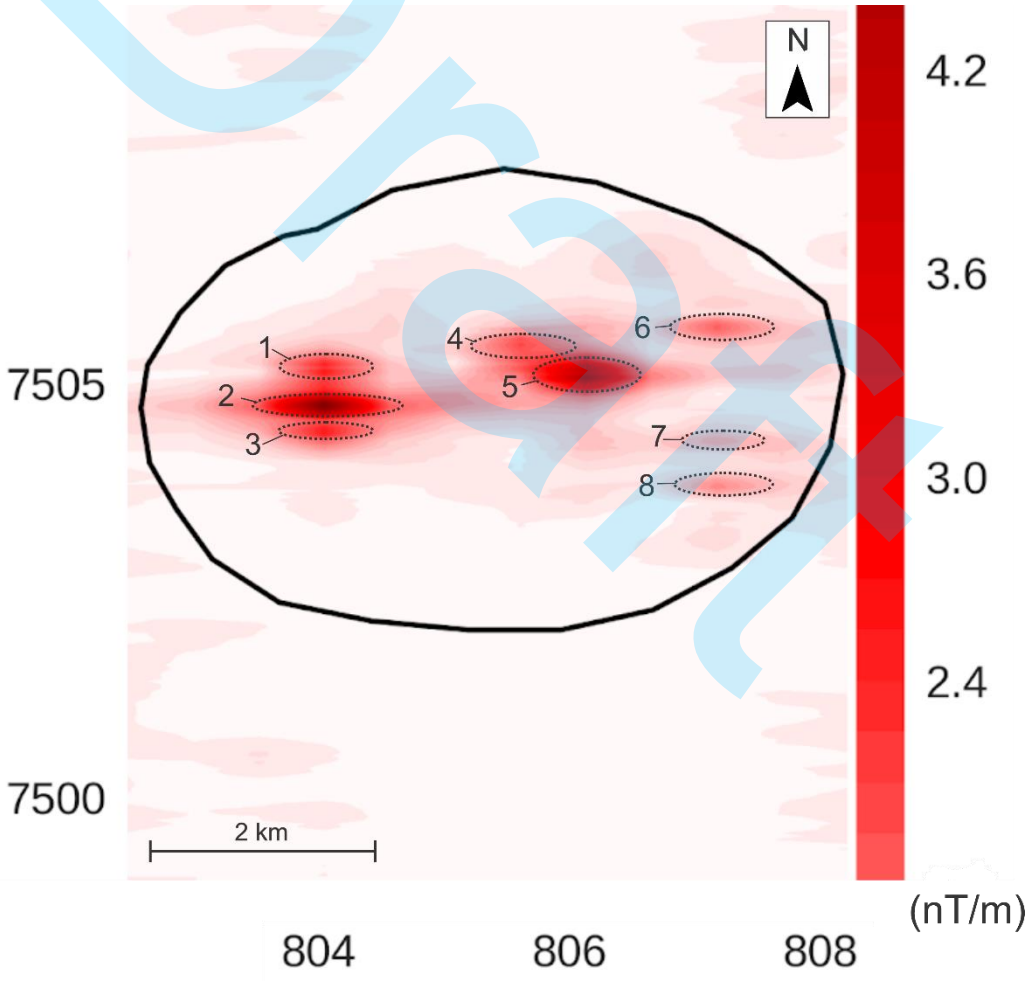

Figure 9: The eight anomalies mapped have high TGA values (nT/m), where one can identify anomalous magnetic sources.

The figure reinforces the hypothesis that the magnetic gradient of the region is composed of multiple anomalous domains. The eight identified anomalous peaks may represent areas with varying concentrations of ferromagnesian minerals or different magmatic bodies within the intrusion, as noted by Li (2006).

For the hypothesis of a single intrusion with magnetic heterogeneity, it is crucial to consider the process of fractional crystallization as a generator of these distinct mineralogical zones (Li, 2006; Chmyz, 2017), which produce detectable magnetic signatures. However, this hypothesis can be dismissed, as authors such as Brotzu et al. (2007) and Fagundes (2024) argue that fractional crystallization was not the primary magmatic evolutionary process of the MSJ, nor responsible for the recorded facies diversity. Consequently, mineralized zones with magnetic minerals, originating from a fractional crystallization process and generating anomalous peaks, are not applicable to the MSJ.

For the hypothesis involving multiple intrusive bodies, the segmentation into eight anomalies may indicate the presence of distinct (non-cogenetic) magmatic intrusions that later interacted during magma mixing events. This idea aligns with the findings of this study, as fundamental methods such as field observations and petrographic analysis already suggest such a process. Furthermore, the aforementioned authors affirm that mechanisms like magma mixing were predominant in the magmatic evolution of the MSJ. Brotzu et al. (2007) and Fagundes (2024) support this assertion through analyses of elemental and isotopic geochemistry. Furthermore, Sales and Martins (2024) identified a magma chamber approximately 4 km beneath the surface through 3D modeling, unveiling features indicative of magmatic processes, including magma mixing and crustal assimilation.

A relevant factor to discuss is the distribution of the peaks. The moderately linear and aligned arrangement of the anomalies suggests they may be related to some structural control or magmatic process, such as fractures or magma feeding channels. The 3D model proposed by Sales and Martin (2024) reveals that the complex is associated in the subsurface with magnetic lineaments of NW-SE and NE-SW direction, which confirms a structural control on the intrusion.

The combination of textural studies and magnetometric signatures aligns with the models proposed by Davidson et al. (2007). These authors link textures to specific magmatic systems (Figure 10) operating under open- and closed-system regimes. According to Davidson et al. (2007), the textural complexities described in this study suggest that the processes forming the complex are based on a system involving two or more non-cogenetic magmatic centers. These centers evolved over time and became interconnected, producing diverse textures (Figure 10C). This is reflected in clinopyroxene, garnet, and amphibole crystals through irregular and concentric compositional zoning, corroded rims, and the presence of poikilitic texture.

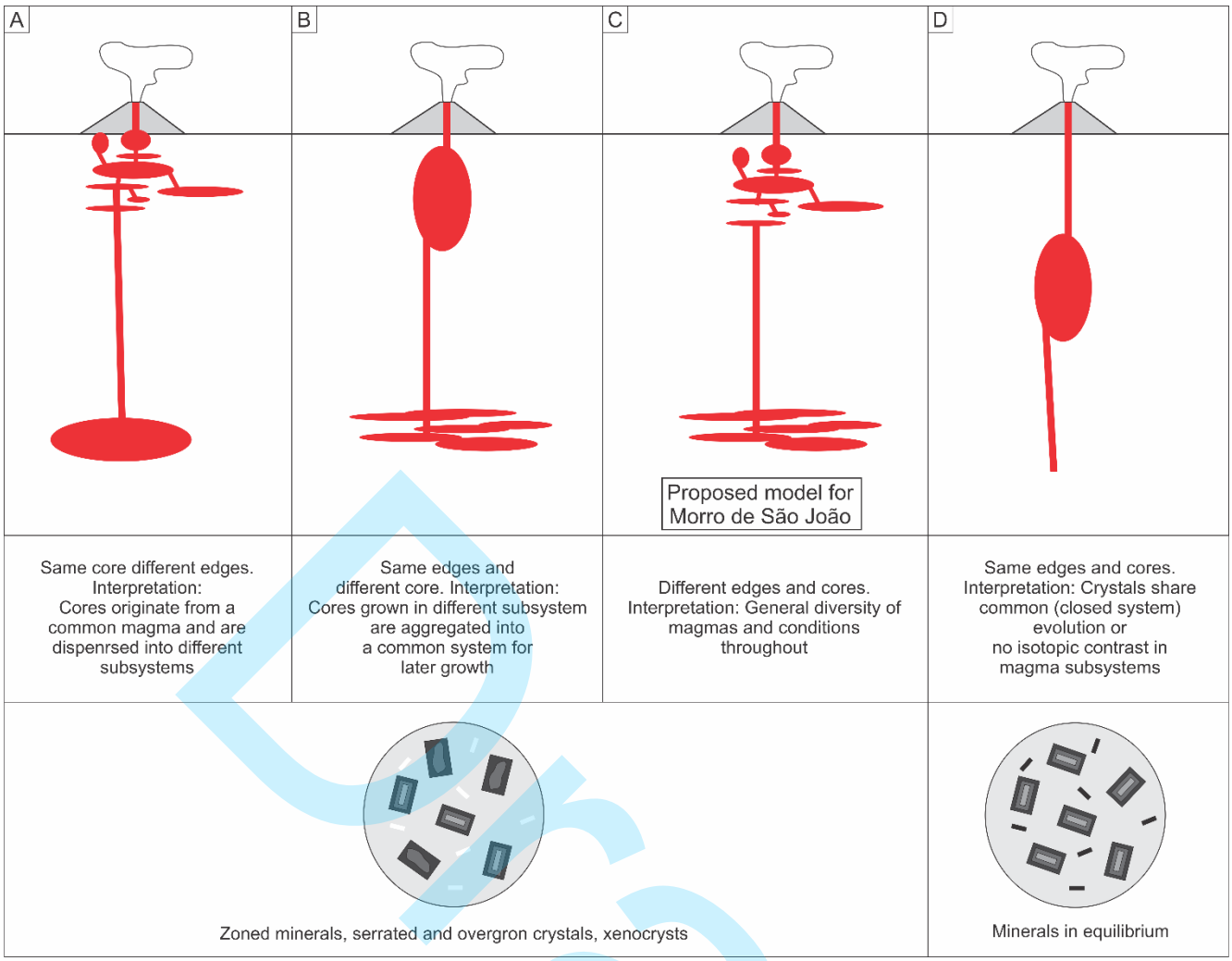

Figure 10: A simplified diagram of magmatic systems, modified from Davidson et al. (2007), shows different forms of mineral zoning and causes of generation.

Thus, it is possible to affirm that the magnetometric signatures, as revealed by the Total Gradient Amplitude Map of the MSJ, support the hypothesis that one of the mechanisms driving the magmatic evolution of the complex involved magma mixing. The various anomalous domains observed in the subsurface can be interpreted as intrusions that were once distinct, non-cogenetic magma batches.

Geodynamic implications

Throughout the processing of magnetometric data, it was observed that the alkaline complex, at the time of its crystallization, was affected by reversed magnetic polarity phenomenon. Figure 11 exhibits the correlation between the geological timetable and the terrestrial geomagnetic polarity table, as presented by Garcés and Beamud (2016). The time scale reveals the normal and reverse polarity periods that occurred during the Paleocene time.

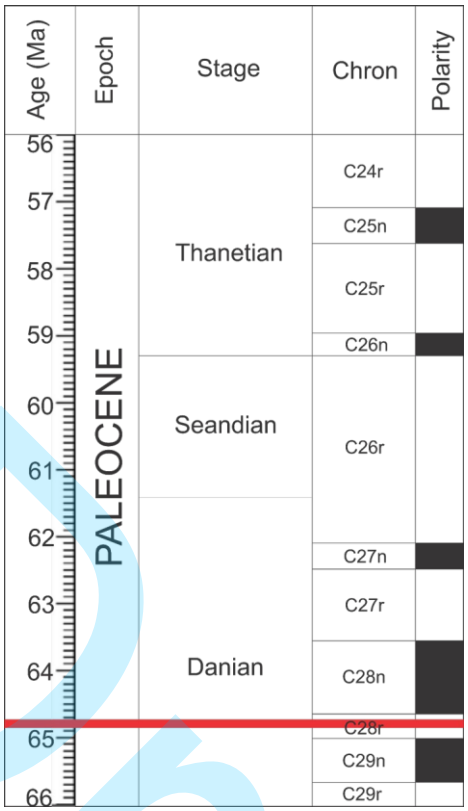

Figure 11: The geological time scale with the geomagnetic polarity of the Paleocene modified by Garcés and Beamud (2016). The dark areas denote periods when the polarity is normal, and the light areas denote periods when the polarity is reversed. The red trace corresponds to the age at which the MSJ crystallized with age, according to Mota et al. (2009).

Reverse polarity arises when the magnetic field changes its orientation so that magnetic north and south are exchanged. These events usually involve a prolonged decline in field strength followed by a rapid recovery after the new orientation is established (Wilson, 1972). The cause of this phenomenon is discussed as major tectonic events that may or may not be associated with the Earth's core (Muller, 2002). These events can include the arrival of portions of continental plate slabs subducted into the deep mantle or the initiation of new mantle plumes from the core-mantle boundary (Dobretsov et al., 2021).

Reversed magnetic polarity determined by the intensity of mantle plumes can lead to the cooling of the core, an increase in the rate of convection in the asthenosphere, and, consequently, changes in the lithosphere (Dobretsov et al., 2021). The same author relates major reversal events to the extrusion of large igneous provinces, such as the Serra Geral - Etendeka, and mass extinctions.

This phenomenon directly implies a discussion of the geodynamic models proposed for the genesis of the MSJ and, consequently, the genesis of the PCCF. In the current literature, there are three hypotheses of a combined model between the movement of a hotspot under the South American

plate in a NW-SE direction (Herz, 1977; Thomaz Filho and Rodrigues, 1999; Marsh, 2006); mantle plume activity (Thompson et al., 1998); and (3) subcrustal faults (Almeida, 1991; Riccomini et al., 2005) generating adiabatic decompression and, consequently, magmatism.

The hot spot plume model is not validated within the PCCF, as there is a lack of linear geochronological progression associated with alkaline intrusions. Furthermore, recent studies employing U-Pb zircon dating (Carvalho et al., 2023; Teodoro et al., 2025; Fagundes, 2024) have confirmed the absence of a downward age progression along the trend.

The hypothesis of the plume as a heat supplier is coherent, since authors (Sleep, 1990; Condie, 1997; Mota, 2012) estimate that for the head of a deep mantle plume, i.e., a plume generated at the core-mantle interface, the dimensions are around 1,000 to 1,500 km in diameter. If this is correct, it is possible, using heat convection, to generate magmatism in distant locations with similar ages and isotopic compositions (Sonoki and Garda, 1988; Thompson et al., 1998; Ulbrich et al., 2003; Motoki et al., 2013; Rosa and Rubeti, 2018), although they are petrographically distinct. This may explain the decreasing non-linearity of the ages and the geochemical similarities of the ages of the bodies belonging to the PCCF.

The model also recognizes that a first phase of alkaline magmatism was generated during extensional events related to the break-up of the Gondwana paleocontinent (Almeida, 1967). A second phase of alkaline magmatism was associated with the formation of the CRSB in the Lower Cretaceous (Riccomini et al., 2004). This whole process would have generated a decompression of the subcontinental lithospheric mantle which, combined with the heat coming from the plume, allowed magma to form and be injected into the crust.

In the PCCF, the Poços de Caldas Alkaline Massif also shows signatures of the reversed geomagnetic polarity phenomenon (Marangoni and Mantovani, 2013). However, extending this reasoning to the other bodies of the PCCF is hasty, as there are no studies of their magnetometric signatures. In the southeast, studies of the magnetic signatures of alkaline igneous provinces are concentrated only on the bodies of the Ponta Grossa High documented by Gomes et al. (2011) and Marangoni and Mantovani (2013).

CONCLUSIONS

The results obtained in this study underscore the significance of magma mixing processes in the evolution of the Morro de São João Alkaline Complex (MSJ). The integration of petrographic and magnetometric data highlights that the textural and compositional diversity of the MSJ rocks is closely linked to the interaction between distinct magmatic pulses in an open-system environment. Textures such as the poikilitic texture observed in amphibole crystals serve as significant petrographic indicators of these interaction processes.

The distribution of anomalous domains identified on the Total Gradient Amplitude (TGA) map supports the hypothesis of multiple intrusive magmatic bodies that are non-cogenetic and interacted during magma mixing events. Furthermore, the magnetic signatures provide a new perspective on the

structural heterogeneity of the MSJ, emphasizing the potential influence of structural controls such as fractures or magma feeding channels.

From a geodynamic perspective, the data suggest that the complex was influenced by geomagnetic polarity reversal phenomena associated with mantle plume activity and extensional tectonic processes related to the Gondwana break-up. These processes contributed to the generation of alkaline magmatism in distinct phases, driven by the decompression of the subcontinental lithospheric mantle and the thermal influence of deep mantle plumes.

ACKNOWLEDGEMENTS

We thank the Laboratório de Estudos Tectônicos - LET/Tektos (UERJ), coordinated by Professor Júlio Almeida/UERJ for technical support; the Laboratório de Modelagem e Evolução Geológica coordinated by Professor Sérgio Valente/UFRRJ for technical support. Additional funding was provided by CAPES (Postdoctoral Fellowship, Process No. 88881.177228/2018-01), FAPERJ APQ1 (Project No. 210.179/2019), FAPERJ EMERGENTES Emergentes (E-26/010.002147/2019) and FAPERJ JCNE 2022 (Process No. E-26/201.469/2022). We thank CNPQ PQ (Process No. 304837/2021-0), CNPQ Museus (Process No. 407628/2022-3), CNPQ PROTRINDADE (Process No. 441837/2024-7) and CNPQ INCT Instituto GeoAtlantico (Process No. 58/20222405653/2022-0) for all support. PETROMAGMATISMO-PETROBRAS (2017/0035-1) coordinated by Professor Sérgio Valente/UFRRJ for the financial support.

REFERENCES

Almeida, F.F.M., 1983, Relações tectônicas das rochas alcalinas mesozoicas da região meridional da Plataforma Sulamericana. Revista Brasileira de Geociências, 13 (3):139- 158.

Almeida, F. F. M., 1967, Origem e evolução da Plataforma Brasileira. Boletim 241, Rio de Janeiro: DNPM-Divisão de Geologia e Mineralogia, p. 36.

Almeida, F. F. M., 1991, O alinhamento magmático de Cabo Frio. 2o Simpósio de Geologia do Sudeste, São Paulo, Atas, p. 423–428.

Almeida, J. C. H., Heilbron, M., Schmitt, R., Valeriano, C. M., Rubim, I. N., Mohriak, W. U., Júnior, D. L. M., Tetzner, W., 2013, Guia de campo na área continental do Alto de Cabo Frio. Boletim de Geociências. Petrobras, 21, 325-355.

Alves, A., Janasi, V. de A., Neto, M. C. C., 2016, Sources of granite magmatism in the Embu Terrane (Ribeira Belt, Brazil): Neoproterozoic crust recycling constrained by elemental and isotope (Sr-Nd-Pb) geochemistry. Journal of South American Earth Sciences, v. 68, p. 205–223. https://doi.org/10.1016/j.jsames.2015.10.014

Azzone, R.G., Muñoz, P.M., Enrich, G.E.R., Alves, A., Ruberti, E., Gomes C.B. 2016. Petrographic, geochemical and isotopic evidence of crustal assimilation processes in the Ponte Nova alkaline mafic–ultramafic massif, SE Brazil. Lithos, 260:58-75. https://doi.org/10.1016/j.lithos.2016.05.004

Baranov, V., 1957, A new method for interpretation of aeromagnetic maps pseudo-gravimetric anomalies: Geophysics, 22, 359–383. https://doi.org/10.1190/1.1438369

Barros, T. M. J., Brito, P. C., Corval, A., Valente, S. C., Miranda, A, W, A., 2023, The post-breakup magmatism in Cabo Frio High, Campos Basin, Brazil: implications to a thinned lithosphere contribution in magma formation. Comunicações Geológicas. 110, 1, 39 - 60. https://doi.org/10.34637/h145-3n13

Bilim, F., Ates, A., 2004, An enhanced method for estimation of body magnetization direction from pseudogravity and gravity data: Computers & Geosciences, 30, 161–171. https://doi.org/10.1016/j.cageo.2003.09.003

Blakely, R. J., 1996, Potential theory in gravity and magnetic applications. Cambridge: Cambridge University Press, 464 pp.

Brotzu, P., Melluso, L., Bennio, L., Gomes, C. B., Lustrino, M., Morbidelli, L., Morra, V., Ruberti, E., Tassinari, C., D'Antonio, M., 2007, Petrogenesis of the Early Cenozoic potassic alkaline complex of Morro de São João, southeastern Brazil. Journal of South American Earth Sciences, v. 24, n. 1, p. 93–115. https://doi.org/10.1016/j.jsames.2007.02.006

Carvalho, M, O., Mottramd, C. M., Valeriano, C. M., Ramos, R. C., Parrish, R., Dunlop, J., Cota, N., Paravidini, G., Neto, C. C. A., Heilbron, M., Storey, C., 2023, Sedimentary provenance in continental rifts: U–Pb detrital zircon, Nd and Sr isotopes and lithogeochemistry of the Eocene alluvial sandstones of the Resende Basin, SE–Brazil. Sedimentary Geology 453, 106452. https://doi.org/10.1016/j.sedgeo.2023.106452

Chmyz, L., Arnaud, N., Biondi, J.C., Azzone, R.G., Bosch, D., Ruberti, E., 2017, Ar-Ar ages, Sr-Nd isotope geochemistry, and implications for the origin of the silicate rocks of the Jacupiranga ultramafic-alkaline complex (Brazil). J. South Am. Earth Sci., 77:286-309. https://doi.org/10.1016/j.jsames.2017.05.009

Clark, D. A., 2014, Methods for determining remanent and total magnetisations of magnetic sources - A review. Exploration Geophysics, 45(4), 271–304. https://doi.org/10.1071/eg14013

Condie, K. C., 1997, Plate Tectonics and Crustal Evolution. 4 ed. Oxford-UK: Butterworth-Heinemann, 282 p. https://doi.org/10.1016/B978-0-7506-3386-4.X5000-9.
CPRM, 2012, Projeto Aerogeofísico Rio de Janeiro. Relatório Final do Levantamento e processamento dos dados magnetométricos e gamaespectrométricos. Prospector Aerolevantamentos e Sistemas Ltda. Volume I. Programa Geologia do Brasil PGB.

Dannemiller, N., Li, Y., 2006, A new method for determination of magnetization direction. Geophysics, 71(6), L69–L73. https://doi.org/10.1190/1.2356116

Davidson, J.P., Morgan, D.J., Charlier, B.L.A., Harlou, R., Hora, J.M., 2007, Microsampling and isotopic analysis of igneous rocks: implications for the study of magmatic systems: Annual Review of Earth and Planetary Sciences, v. 35, p. 273-311. https://doi.org/10.1146/annurev.earth.35.031306.140211

Dobretsov, N., Metelkin, D., Vasilevskiy, A., 2021, Typical Characteristics of the Earth's Magnetic and Gravity Fields Related to Global and Regional Tectonics. Russian Geology and Geophysics, 62, 6-24. https://doi.org/10.2113/RGG20204261

Dunlop, D.J., Özdemir, Ö., 1997, Rock Magnetism: Fundamentals and Frontiers. Cambridge University Press, 573 pp. https://doi.org/10.1017/CBO9780511612794

Dutra, A. C. D., Guimarães, S. N. P., Salomão, M. S., Palermo, N., Bertolino, L. C., Bruno, H., Mane, M. A., 2022, Use of Airborne Geophysics for Potential Fe-Ti-V Oxides Mineralization in Metagabbros: An Example within the Paleoproterozoic Basement of Ribeira Belt, Southeast Brazil. Brazilian Journal of Geophysics. v. 40, 2, 1-24. https://doi.org/10.22564/brjg.v40i2.2161

Fagundes, M. B., 2020, Caracterização Petrológica e Geoquímica do Complexo Alcalino do Morro de São João, Casimiro de Abreu-RJ. M.Sc. dissertation, Universidade do Estado do Rio de Janeiro, Brasil. p.116.

Fagundes, M. B., 2024, Petrogênese, evolução magmática do Complexo Alcalino do Morro de São João, sudeste do Brasil, e suas implicações na evolução da Plataforma Sul-Americana. Ph.D. Thesis, Universidade do Estado do Rio de Janeiro, Brazil, p.337.

Fagundes, M. B., Santos, A. C., Geraldes, M. C., Valente, S. C., Guedes, E., Barbosa, T. R. P., Lopes, J. C., 2024, Petrological implications of melanite in the rocks of the Morro de São João Alkaline Complex, Casimiro de Abreu, Rio de Janeiro, Brazil. Brazilian Journal of Geology, 54(3),

e20240016. https://doi.org/10.1590/2317- 4889202420240016

Fedi, M., Floria, G., Rapolla, A., 1994, A method to estimate the total magnetization direction from a distortion analysis of magnetic anomalies. Geophysical Prospecting, 42(3), 261–274. https://doi.org/10.1111/j.1365-2478.1994.tb00209.x

Garcés, M., Beamud, E., 2016, La Magnetoestratigrafía y la Escala del Tiempo Geológico basada en las inversiones del campo magnético terrestre. Enseñanza de las Ciencias de la Tierra, v.24, n.3, 282-293. https://raco.cat/index.php/ECT/article/view/328854

GEOSGB, 2022, Dados, Informações e Produtos do Serviço Geológico do Brasil. Disponível em <4. Acesso em: Jan/2022. Available at <http://geosgb.cprm.gov.br>. Accessed on: Jan/2022.

Gerovska, D., M. J. Araúzo-Bravo, and P. Stavrev, 2009, Estimating the magnetization direction of sources from southeast Bulgaria through correlation between reduced-to-the-pole and total magnitude anomalies: Geophysical Prospecting, 57, 491–505. https://doi.org/10.1111/j.1365-2478.2008.00761.x

Gonzalez, S. P., Barbosa, V. C. F., and Oliveira, Jr., V. C., 2022, Analyzing the ambiguity of the remanent magnetization direction separated into induced and remanent magnetic sources. Journal of Geophysical Research: Solid Earth, 127, e2022JB024151. https://doi.org/10.1029/2022JB024151

Gomes, C. B., Ruberti, E., Comin-Chiaramonti, P., Azzone, R. G., 2011, Alkaline magmatism in the Ponta Grossa Arch , SE Brazil : A review. Journal of South American Earth Sciences, 32(2), 152-168. https://doi.org/10.1016/j.jsames.2011.05.003

Harris, C.R., Millman, K.J., van der Walt, S.J., Gommers, R., Virtanen, P., Cournapeau, D., Wieser, E., Taylor, J., Berg, S., Smith, N. J., Kern, R., Picus, M., Hoyer, S., van Kerkwijk, M. H., Brett, M., Haldane, A., del Río, J. F., Wiebe, M., Peterson, P., Gérard-Marchant, P., Sheppard, K., Reddy, T., Weckesser, W., Abbasi, H., Gohlke, C., Oliphant, T. E., 2020, Array programming with NumPy. Nature, 585, 357–362. https://doi.org/10.1038/s41586-020-2649-2

Heilbron, M., Pedrosa-Soares, A.C., Campos Neto, M., Silva, L.C., Trouw, R.A.J., Janasi, V.C, 2004, A Província Mantiqueira. In: V. Mantesso-Neto, A. Bartorelli, C.D.R. Carneiro, B.B. Brito Neves (eds.) O Desvendar de um Continente: A Moderna Geologia da América do Sul e o Legado da Obra de Fernando Flávio Marques de Almeida. São Paulo, Ed. Beca, cap. XIII, p. 203-234.

Heilbron, M., Eirado, L. G., Almeida, J., 2016, Geologia e Recursos Minerais do Estado do Rio de Janeiro. Nota Explicativa - CPRM, p. 109.

Herz, N.,1977, Timing of spreading in the South Atlantic: Information from Brazilian alkalic rocks. Geological Society of America Bulletin, 88, 1, 101-112. https://doi.org/10.1130/0016-7606(1977)88%3C101:TOSITS%3E2.0.CO;2

Hill, G., Moorkamp, M., Avram, Y., Hogg, C., Mateschke, K., Gahr, S., Schultz, A., Bowles-Martinez, E., Peacock, J., Karcioglu, G., Chen, C., Cimarelli, C., Carrichi, L., Ogawa, Y., 2023, Probing the 4D evolution of active magmatic systems through magnetotelluric monitoring, EGU General Assembly, EGU23-2969, 24–28. https://doi.org/10.5194/egusphere-egu23-2969, 2023

Huang, H., Fraser, D. C., 2001, Airborne resistivity and susceptibility mapping in magnetically polarizable areas. Geophysics, 65(2), 502–511. https://doi.org/10.1190/1.1444744

Jian, X., Liu, S., Hu, X., Zhang, Y., Zhu, D., and Zuo, B., 2022, A new method to estimate the total magnetization direction from the magnetic anomaly: Multiple correlation. Geophysics, 87 (5): G115–G135. doi: https://doi.org/10.1190/geo2021-0733.1

Latypov, R. M., Yu Chistyakova, S., Namur, O., Barnes, S., 2020, Dynamics of evolving magma chambers: textural and chemical evolution of cumulates at the arrival of new liquidus phases. Earth-Science Reviews, v. 210. https://doi.org/10.1016/j.earscirev.2020.103388

Le Maitre, R. W., 2002, Igneous Rocks: A Classification and Glossary of Terms: A Classification and Glossary of Terms. Cambridge University Press. 2nd ed., 236 pp. https://doi.org/10.1017/CBO9780511535581.

Lelièvre, P. G., Oldenburg, D. W., 2009, A 3D total magnetization inversion applicable when significant, complicated remanence is present. Geophysics, 74(3), L21–L30. https://doi.org/10.1190/1.3103249

Li, J., Y. Zhang, G. Yin, H. Fan, and Z. Li, 2017, An approach for estimating the magnetization direction of magnetic anomalies: Journal of Applied Geophysics, 137, 1–7. https://doi.org/10.1016/j.jappgeo.2016.12.009

Li, X., 2006, Understanding 3D analytic signal amplitude. Geophysics, vol. 71, no. 2, B13–B16. https://doi.org/10.1190/1.2184367

Magee, C., Stevenson, C. T. E., Ebmeier, S. K., Keir, D., Hammond, O. S., Gottsmann, J, H., Whaler, K, A., Schofield, N., Jackson, C. A-L., Petronis, M. S., O'Driscoll, B., Morgan, J., Cruden., A.,

Vollgger., A. A., Dering, G., Micklethwaite, S., Jackson, M. D., 2018, Magma Plumbing Systems: A Geophysical Perspective. Journal of Petrology, Vol. 59, No. 6, 1217–1251. https://doi.org/10.1093/petrology/egy064

Matos, C. A. de, & Mendonca, C. A., 2020, Poisson magnetization-to-density-ratio and magnetization inclination properties of banded iron formations of the Carajás mineral province from processing airborne gravity and magnetic data. Geophysics, 85(5), K1-K11. https://doi.org/10.1190/geo2019-042.1

Marangoni, Y, R., Mantovani, M. S. M., 2013, Geophysical Signatures of the alkaline intrusions bordering the Paraná Basin. Journal of South American Earth Sciences. v41, p.p. 83-98. https://doi.org/10.1016/j.jsames.2012.08.004

Marsh, B.D., 2006, Dynamics of magmatic systems. Elements, 2(5):287-292. https://doi.org/10.2113/gselements.2.5.287

Mazaud, A., 2007, Geomagnetic Polarity Reversals. In D. Gubbins & E. Herrero-Bervera (Eds.), Encyclopedia of geomagnetism and paleomagnetism (pp. 320–324). Dordrecht: Springer Netherlands.

Mohriak, W. U., Almeida, J. C. H., Gordon, A. C. (2022). South Atlantic Ocean: postbreakup configuration and Cenozoic magmatism. In: Meso-Cenozoic Brazilian Offshore Magmatism. Academic Press. 1-45. https://doi.org/10.1016/B978-0-12-823988-9.00007-1

Mota, C.E.M., 2012, Petrogênese e geocronologia das intrusões alcalinas de Morro Redondo, Mendanha e Morro de São João: caracterização do magmatismo alcalino no estado do Rio de Janeiro e implicações geodinâmicas. Ph.D. thesis. Universidade do Estado do Rio de Janeiro, Brazil. 203 pp.

Mota, C.E.M., Geraldes, M. C., de Almeida, J. C. H., Vargas, T., de Souza, D. M., Loureiro, R. O., da Silva, A. P., 2009, Características Isotópicas (Nd e Sr), Geoquímicas e Petrográficas da Intrusão Alcalina do Morro do São João: Implicações Geodinâmicas e Sobre a Composição do Manto Sublitosférico. Geologia USP - Série Científica, São Paulo, 9, n. 1, 85-100. https://doi.org/10.5327/Z1519-874X2009000100006

Motoki, A., Araujo, A. N., Geraldes, M. C., Jourdan, F., Motoki., K. F., Silva, S., 2013, Nepheline syenite magma differentiation with Continental crustal assimilation for the Cabo Frio Island Intrusive Complex, State of Rio de Janeiro, Brazil. Geociências. 32(2): 195-218.

Mollo, S., Hammer, J. E., 2017, Dynamic crystallization in magmas. EMU Notes in Mineralogy, 6, 373-418. https://doi.org/10.1180/EMU-notes.16.12

Muller, R. A, 2002, Avalanches at the core-mantle boundary». Geophys. Res. Lett. 29 (19). https://doi.org/10.1029/2002GL015938

Nabighian, M. N., 1972, The analytic signal of two-dimensional magnetic bodies with polygonal cross-section - Its properties and use for automated anomaly interpretation: Geophysics, 37, 3, 507–517. https://doi.org/10.1190/1.1440276.

Nabighian, M. N., 1974, Additional comments on the analytic signal of two-dimensional magnetic bodies with polygonal cross-section: Geophysics, 39,1, 85-92. https://doi.org/10.1190/1.1440416

Nabighian, M. N, Grauch, V. J. S., Hansen, R. O., LaFehr, T. R., Li, Y., Peirce, J. W., Phillips, J. D., and Ruder, M. E., 2005, The historical development of the magnetic method in exploration. Geophysics, 70:6 33ND-61ND. https://doi.org/10.1190/1.2133784

Oliveira Jr., V. C., Sales, D. P., Barbosa, V. C. F., Uieda, L., 2015, Estimation of the total magnetization direction of approximately spherical bodies. Nonlinear Processes in Geophysics, 22(2), 215–232. https://doi.org/10.5194/npg-22-215-2015

Ravat, D., 2007, Crustal magnetic field. In D. Gubbins & E. Herrero-Bervera (Eds.), Encyclopedia of geomagnetism and paleomagnetism (pp. 140–144). Dordrecht: Springer Netherlands. https://doi.org/10.1007/978-1-4020-4423-6_5

Reid, A., 2012, Forgotten truths, myths and sacred cows of Potential Fields Geophysics - II, in SEG Technical Program Expanded Abstracts 2012, pp. 1-3, Society of Exploration Geophysicists. https://doi.org/10.1190/segam2012-0178.1

Reis, A. L. A., Oliveira Jr., V. C., and Barbosa, V. C. F., 2020, Generalized positivity constraint on magnetic equivalent layers. Geophysics, 85(6), J99–J110. https://doi.org/10.1190/geo2019-0706.1

Ribeiro-Filho, N., Bijani, R., Ponte-Neto, C., 2020, Improving the crosscorrelation method to estimate the total magnetization direction vector of isolated sources: A space-domain approach for unstable inclination values. Geophysics, 85(4), J59–J70. https://doi.org/10.1190/geo2019-0008.1

Riccomini, C., Sant'Anna, L.G., Ferrari, A.L., 2004, Evolução geológica do Rift Continental do Sudeste do Brasil. In: Mantesso-Neto V., Bartorelli A., Carneiro C.D.R., Britto-Neves B.B. (Org.) Geologia do Continente Sul-americano: Evolução da obra de Fernando Flávio Marques de Almeida.

Beca, São Paulo, 647 p.

Riccomini, C.; Velázquez, V. F.; Gomes, C. B., 2005, Tectonic Controls of the Mesozoic and Cenozoic Alkaline Magmatism in Central-Southeastern Brazilian Platform. In: Comin-Chiaramonti, P., Gomes, C. Mesozoic to Cenozoic alkaline magmatism in central-southeastern Brazilian Platform. Editora da Universidade de São Paulo. 2017, p. 31–55.

Roest, W. R., Pilkington, M., 1993, Identifying remanent magnetization effects in magnetic data. Geophysics, 58(5), 653–659. https://doi.org/10.1190/1.1443449

Rosa, P.A. da S., Ruberti, E., 2018, Nepheline syenites to syenites and granitic rocks of the Itatiaia Alkaline Massif, Southeastern Brazil: new geological insights into a migratory ring Complex. Brazilian Journal of Geology. 48, 347–372. https://doi.org/10.1590/2317-4889201820170092

Sadowski, G.R., Dias Neto, C.M., 1981, O lineamento sismo-tectônico de Cabo Frio. Revista Brasileira de Geociências, v. 11, no. 4, p. 209-212. https://doi.org/10.25249/0375-7536.1981209212

Sales, T. J. B., Martins, S. S, 2024, Aeromagnetic geophysical data 3D inversion: Revealing internal and external structures of Morro São João Alkaline Complex, Southeast Brazil. Journal of South American Earth Sciences, 144, 105008. https://doi.org/10.1016/j.jsames.2024.105008

Schmitt, R.S., Trouw, R.A.J., Schmus, W.R.V., Pimentel, M. M., 2004, Late amalgamation in the central part of Western Gondwana: new geochronological data and the characterization of a Cambrian collision orogeny in the Ribeira Belt (SE Brazil).Precambrian Research, 133:29-61. https://doi.org/10.1016/j.precamres.2004.03.010

Sharma, P.V., 1987, Magnetic Method applied to mineral exploration: Ore Geology Reviews, 2(4), 323–357. https://doi.org/10.1016/0169-1368(87)90010-2

Sleep, N. H., 1990, Hot-spots and mantle plumes: Some phenomenology. Journal of Geophysical Research, v. 95, p. 6715-6736. https://doi.org/10.1029/JB095iB05p06715

Sonoki, I.K., Garda. G. M., 1988, Idades K-Ar de rochas alcalinas do Brasil Meridional e Paraguai Oriental: compilação e adaptação às novas constantes de decaimento. Bol. IG-USP, Cien., v. 19, p. 63–85. https://doi.org/10.11606/issn.2316-8986.v19i0p63-85

Streckeisen, A.L. 1976. Classification and Nomenclature of Igneous Rocks. Neues Jahrbuch für Mineralogie, 107, 144-240.

Telford, W. M., Geldart, L. P., Sheriff R. E., 1990, Applied Geophysics, 2nd ed. Cambridge University Press, Cambridge, 770 pp. https://doi.org/10.1017/CBO9781139167932

Teodoro, M. A. M., Santos, A. C., Bertolino, L. C., Rosa, Pedro, A. S., Bezerra, C. R., Monteiro, L. G. P., Lopes, J. C., Fagundes, M. B., Geraldes, M., Cardoso, L. M. C., Jourdan, F., 2025, Poços de Caldas – Cabo Frio Alignment: a Petrochronological Review of an Unconventional Plume Model. Anuário do Instituto de Geociências, https://doi.org/10.11137/1982-3908_2025_48_65281

Thomaz Filho A., Rodrigues A.L., 1999, O alinhamento de rochas alcalinas Poços de Caldas- Cabo Frio (RJ) e sua continuidade na Cadeia Vitória-Trindade. Brazilian Journal of Geology, v. 29 (2), p. 189–194. https://doi.org/10.25249/0375-7536.199929189194

Thompson, R.N., Gibson, S.A., Mitchell, J.G., Dickin, A.P., Leonardos, O.H., Brod, J.A., Greenwood, J.C., 1998, Migrating Cretaceous-Eocene Magmatismin the Serra do Mar Alkaline Province, SE Brazil: Melts from the Deflected Trindade Mantle Plume? Journal of Petrology. 39, 1493–1526. https://doi.org/10.1093/petroj/39.8.1493

Tontini, F. C., Pedersen, L. B., 2008, Interpreting magnetic data by integral moments. Geophysical Journal International, 174(3), 815–824. https://doi.org/10.1111/j.1365-246X.2008.03872.x

Tupinambá, M., Heilbron, M., Valeriano, C., Porto Júnior, R., De Dios, F.B., Machado N., Silva L.G. E., Almeida, J. C. H., 2012, Juvenile contribution of the Neoproterozoic Rio Negro Magmatic Arc (Ribeira Belt, Brazil): Implications for Western Gondwana amalgamation. Gondwana Research, v. 21, p. 422–438. https://doi.org/10.1016/j.gr.2011.05.012

Ulbrich, H.H.G.J., Demaiffe, D., Vlach, S.R.F., Ulbrich, M.N.C., 2003, Geochemical and Sr, Nd and Pb isotope signatures of phonolites and nepheline syenites from Poços de Caldas alkaline massif, southeastern Brazil. 4th South American Symposium on Isotope Geology, Salvador, Short Papers, pp. 698-701.

Valeriano, C., D. E. M., Tupinambá, M., Simonetti, A., Heilbron, M., Almeida, J.C.H., 2011, U-Pb LA-MC-ICPMS geochronology of Cambro-Ordovician post-collisional granites of the Ribeira belt, southeast Brazil: Terminal Brasiliano magmatism in central Gondwana supercontinent. Journal of South American Earth Sciences, v. 32, p. 416– 428. https://doi.org/10.1016/j.jsames.2011.03.003

Ville, J., 1948, Théorie et applications de la notion de signal analytique: Cables et Transmissions, 2A, 61–74.

Virtanen, P., Gommers, R., Oliphant, T.E., Haberland, M., Reddy, T., Cournapeau, D., Burovski, E., Peteron, P., Weckesser, W., Bright, J., vn der Walt, S. J., Brett, M., Wilson, J., Millman, K. J., Mayorov, N., Nelson, A. R. J., Jones, E., Kern, R., Larson, E., Carey, C. J., Polat, I, Feng, Y., Moore, E. W., VanderPlas, J., Laxalde, D., Perktold, J., Cimrman, R., Henriksen, Quintero, E. A., Harris, C. R., Archibald. A. M., Ribeiro, A, H., Pedregosa, F., van Mulbregt, P., SciPy 1.0 Contributors, 2020, SciPy 1.0: fundamental algorithms for scientific computing in Python. Nature Methods, 17, 261–272. https://doi.org/10.1038/s41592-019-0686-2

Vlach, S. R. F., Ulbrich, H. H. G. J., Ulbrich, M. N. C., Vasconcelos, P. M., 2018, Melanite-bearing nepheline syenite fragments and $^{40}Ar/^{39}Ar$ age of phlogopite megacrysts in conduit breccia from the Poços de Caldas Alkaline Massif (MG/SP), and implications. Brazilian Journal of Geology, 48(2), 391-402. https://doi.org/10.1590/2317-4889201820170095

Wilson, R., 1972, Palaeomagnetic Differences Between Normal and Reversed Field Sources, and the Problem of Far-sided and Right-handed Pole Positions. Geophysical Journal International, 28, 295-304. https://doi.org/10.1111/J.1365- 246X.1972.TB06130.X

Zhang, H., D. Ravat, Y. R. Marangoni, G. Chen, and X. Hu, 2018, Improved total magnetization direction determination by correlation of the normalized source strength derivative and the reduced-to-pole fields: Geophysics, 83, no. 6, J75–J85. https://doi.org/10.1190/geo2017-0178.1

Fagundes, M. B.: Main author, study conception and design, data acquisition, result discussion (data analysis and interpretation), manuscript drafting, manuscript critical revision for important intellectual content, version approval of the manuscript to be published, reviews; **Reis, A. L. A.:** Result discussion (data analysis and interpretation), manuscript drafting, review interpretation, effective participation in the adequacy of the manuscript through suggestions from the reviewers together with the main author, version approval of the manuscript to be published, reviews; **Santos, A. C.:** Effective participation in the adequacy of the manuscript through suggestions from the reviewers together with the main author, version approval of the manuscript to be published, reviews; **Geraldes, M. C.:** Effective participation in the adequacy of the manuscript through suggestions from the reviewers together with the main author, version approval of the manuscript to be published, reviews; **Valente, S. C.:** Effective participation in the adequacy of the manuscript through suggestions from the reviewers together with the main author, version approval of the manuscript to be published, reviews; **Gomes, J.:** Study conception and design, result discussion (data analysis and interpretation), version approval of the manuscript to be published, reviews.